

Fracture characteristics and deformation behavior of heterophasic ethylene–propylene copolymers as a function of the dispersed phase composition

P. Doshev^a, R. Lach^a, G. Lohse^b, A. Heuvelsland^b, W. Grellmann^a, H.-J. Radusch^{a,*}

^a*Institute of Materials Science, Martin-Luther University Halle-Wittenberg, D-06099 Halle (Saale), Germany*

^b*Dow Olefinverbund GmbH, D-06258 Schkopau, Germany*

Received 14 February 2005; received in revised form 7 July 2005; accepted 8 July 2005

Available online 10 August 2005

Abstract

The deformation and fracture behavior of in reactor produced heterophasic copolymers, comprising a polypropylene (PP) matrix and an ethylene propylene copolymer (EPC) dispersed phase, have been studied as a function of the dispersed phase composition (ethylene/propylene ratio). Conventional and instrumented Charpy as well as instrumented drop weight tests were employed to quantify the response of the materials to impact loading. Scanning and high-voltage electron microscopy was used for characterization of the deformation mechanisms. Decreasing ethylene content of the EPC led to an enhancement of the matrix/dispersed phase compatibility, reduction of the dispersed phase particle size and therewith to a systematic increase of the impact strength at room temperature and a decrease of the brittle-to-tough transition temperature (T_{BT}) of the materials. The low temperature impact strength was predominantly dependent upon the glass transition temperature of the EPC phase. The results are discussed from the viewpoint of interfacial interactions, size and spatial packing of the dispersed phase domains and the observed deformation mechanisms.

© 2005 Elsevier Ltd. All rights reserved.

Keywords: Polypropylene/ethylene–propylene copolymer blends; Ethylene/propylene ratio; Fracture mechanics parameters

1. Introduction

Polypropylene along with a number of valuable properties exhibits intrinsically brittle behavior under impact loading, especially at low temperatures and high deformation speeds. To overcome this disadvantage, melt blending of suitable elastomers such as ethylene–propylene copolymer (EPC), ethylene–propylene–diene terpolymer (EPDM), styrene–ethylene–butadiene–styrene (SEBS) and recently metallocene ethylene- α -olefin copolymers is most commonly performed [1–4]. However, the impact modification of polypropylene via downstream copolymerization of ethylene and propylene at a certain ratio directly in a reactor cascade is a more effective practice [5,6].

So produced heterophasic copolymers also designated as reactor blends, consist mainly of a polypropylene matrix with embedded ethylene–propylene copolymer (EPC) domains. In dependence on the dispersed phase composition, a certain amount of semi-crystalline ethylene–propylene copolymer is present besides the amorphous EPC [7–9].

The main role of the dispersed modifier particles in the PP/EPC blends is to act as stress concentrators and to relieve the volume strain by cavitation, at the particle/matrix interface as well as within the EPC particles, leading to large plastic deformations of the surrounded matrix [10–17]. In case of polypropylene, the plastic deformation process is interconnected mostly with the formation of crazes, shear bands or shear yielding. They could operate separately or simultaneously in dependence on the temperature and the other test conditions [10,11]. Further on, the size, shape and spatial packing of the dispersed domains, as well as the matrix/dispersed phase compatibility were found to be critical parameters affecting the stress distribution around the particles, their susceptibility to cavitation

* Corresponding author. Tel.: +49 3461 46 2791; fax: +49 3461 46 3891.

E-mail address: hans-joachim.radusch@iw.uni-halle.de (H.-J. Radusch).

and subsequently the brittle-to-tough transition temperature (T_{BTT}) and impact performance of the resulting materials [18]. According to Wu [19], the main material parameter controlling the brittle-to-tough transition in nylon–rubber blends is the interparticle distance (ID). When interparticle distance is smaller than a critical value (ID_c) the material will behave tough, where the ID_c is a parameter characteristic for a given matrix. However, the ID_c was shown to be strongly affected by the temperature and lower interparticle distances reflect in lower T_{BTT} [20,21]. Further on, the intrinsic properties of the dispersed phase, testing method and loading rate are reported to influence the critical interparticle distance as well [22–25].

Despite the interparticle distance model proposed by Wu was found to be applicable for diverse polymer systems its physical explanation is still disputable. Stress field overlap of neighboring particles, changes from plane strain to plane stress conditions in the matrix ligaments and recently stabilization of the dilatational band propagation below the critical interparticle distance are some of the mostly discussed mechanisms [19,26,27].

The fracture toughness of both mechanical and reactor PP/EPC blends has been the subject of extensive studies, focused to the effect of matrix and dispersed phase molecular weight, particle size, interparticle distance and volume fraction of the EPC [28–42]. Nevertheless, the influence of the dispersed phase composition on the impact performance of such blends is only scarcely reported [39,40] or accounted by some authors as negligible [41,42]. In a another study of our group [43,44] it was reported that the compatibility between the components of the heterophasic ethylene–propylene copolymers as well as the dimension of the dispersed domains is primarily controlled by the EPC ethylene content by keeping constant the intrinsic properties and the fraction of the blend components. The increase of propylene content of the ethylene–propylene copolymer was found to enhance the interfacial interaction of the phases and to produce a strong refinement of the dispersed particle size.

Further on, at extremely high propylene content, i.e. low ethylene content of the dispersed phase, a phenomenon of glass transition temperature merging of the both phases has been observed, suggesting high a extent of compatibility.

The objective of the present work is the investigation of the effect of the structural and morphological changes resulting from the EPC composition variation on the impact resistance of the PP/EPC reactor blends. The deformation mechanisms associated with the toughening effect as well as the brittle-to-tough transition are discussed.

2. Experimental

2.1. Materials

The heterophasic copolymers used in this study were research materials provided by Dow Chemical (Schkopau,

Germany). They were produced via sequential polymerization process in a reactor cascade by means of commercial, fourth generation Ziegler–Natta catalyst supported on spherical MgCl_2 . In the first stage a polypropylene homopolymer was synthesized in liquid propylene as a reaction medium. In a next stage, copolymerization of ethylene and propylene at certain ratio takes place in gas phase. Further on, the materials were compounded with a standard additive package in a single screw extruder Plasticorder PL 2100 (Brabender) at 100 rpm and barrel zone temperatures from 210 to 230 °C. The test specimens were produced via an injection molding machine BA 100 (Battenfeld) at barrel temperature of 200 °C and mold temperature of 40 °C.

The ethylene content of the ethylene–propylene copolymer (E_c^{EPC}) was used for characterization of the EPC composition. The E_c^{EPC} represents the weight percentage of ethylene in the gas phase reactor as determined by gas chromatography. The E_c^{EPC} was the main parameter varied during the investigation and, therefore, the studied materials were abbreviated as PP/EP and a number corresponding to the ethylene content of EPC.

Since the amount of elastomer phase in the reactor blends cannot be controlled directly, only a qualitative measure is possible illustrated by the amount of the xylene soluble fraction (XS) in wt%. The XS was measured in boiling xylene according to ASTM D5492. The low isotacticity matrix fraction present in XS is excluded by precipitation with acetone. It should be mentioned that the XS value does not register the semi-crystalline EPC, which would lead to a slight underestimation of the elastomer loading, especially at very low and very high ethylene content.

The molecular parameters of the PP were reflected by the melt flow rate of the PP matrix (MFR^{PP}) determined according to ISO 1133 and were kept constant within the series. The molecular weight of the EPC phase is represented by intrinsic viscosity ($[\eta]^{\text{EPC}}$), measured on the XS fraction. The $[\eta]^{\text{EPC}}$ was determined at 135 °C using decaline as solvent.

The glass transition temperatures of the EPC (T_g^{EPC}) and PP (T_g^{PP}) phases were measured using torsion pendulum with frequency 1 Hz and heating rate 1 K/min as described in detail in another studies [43,44]. Table 1 discloses the main characteristics of the investigated materials.

2.2. Characterization methods

2.2.1. Analyses of morphology and microdeformation

Morphology observations were accomplished by means of a scanning electron microscope JSM 6300 (Jeol). Micrographs were taken from sections of the injection molded dumbbell specimens. The sections were subject to permanganic etching [45] in order to degrade the amorphous ethylene–propylene copolymer and gold-coated before viewing. The weight average diameter of the EPC domains

Table 1
Material Characteristics

Materials	MFR ^{PP} (g/110 min) ^a	MFR ^{Blend} (g/10 min) ^a	XS (wt%) ^b	[η] ^{EPC} (dl/g) ^c	E _c ^{EPC} (wt%) ^d	T _g ^{EPC} (°C) ^e	T _g ^{PP} (°C) ^e	D _w (μm) ^f
PP/EP82	~20	4.7	20.4	3.4	82	-37	20	4.5
PP/EP70	~20	8.1	20.5	2.4	70	-51	19	1.7
PP/EP50	~20	9.4	20.3	2.5	50	-51	16	1.4
PP/EP30	~20	11.1	19.2	2.4	30	-35	12	1.0
PP/EP17	~20	9.7	25.2	1.6	17	10 ^g		0.2

^a Melt flow rate according to ISO 1133.

^b Xylene soluble fraction according to ASTM D5492.

^c Intrinsic viscosity of EPC measured in decalin at 135 °C.

^d Ethylene content of EPC.

^e Glass transition temperature of the EPC and PP phases.

^f Weight average diameter of the EPC particles.

^g Joint glass transition peak at 10 °C.

(D_w) was determined using image analyzing software Qwin (Leica) and given in Table 1.

To quantify the deformation mechanisms taking place in the investigated materials, the fracture surfaces obtained from the instrumented impact test were examined by means of scanning electron microscope JSM 35 C (Jeol) after gold coating.

The micromechanical behavior was studied in a high-voltage electron microscope (HVEM JEOL 1000) operated at 1000 kV. Semi-thin sections of about 1 μm were cut from the bulk material using an ultramicrotome MT-7 (RMC). Each section was fixed between two adhesive tapes and transferred into a special miniature tensile desk. After transferring, the tapes were cut and the self-supported semi-thin sections were deformed up to definite elongation either outside the HVEM under light microscope control or 'in situ' inside the HVEM.

2.2.2. Tensile testing

The uniaxial tensile properties of the materials were measured using tensile testing machine 1425 (Zwick) with cross-head speed of 50 mm/min at room temperature according to ISO 527.

2.2.3. Fracture mechanics testing

For initial assessment of the fracture response, a conventional impact testing was performed at a Charpy device (Zwick 5102) using single edge notched bend (SENB) specimens with dimensions length (L) × width (W) × thickness (B) of 80 × 10 × 4 mm³ according to ISO 179, having a 2 mm deep machined blunt notch. Nevertheless, the impact strength a_{cN} as an integral measure of the total work up to break gives no information about the energy components (elastic and plastic deformation energies, crack arrest/crack propagation energy), the fracture events such as the onset of stable or unstable crack growth, and which role load and deflection play in the fracture process.

Thus, for complete quantification of the fracture behavior of the materials, an instrumented Charpy impact tester with

a maximum work capacity of 4 J pendulum was employed. The same specimen geometry as for the conventional impact testing was used. The testing was performed by pendulum speed of 1.5 m/s and support span (s) of 40 mm in a temperature range from 0 to 80 °C. In order to obtain the brittle-to-tough transition, the tests were conducted by at least five different temperatures for each material. Single edge blunt notch was first machined in the center of the bars and subsequently sharpened by a razor blade. The total notch length (a) was around 2 mm resulting in a relatively small a/W ratio of $a/W \sim 0.2$ causing a higher crack instability than higher a/W . The investigated failure behavior of the PP/EPC reactor blends was characterized by means of fracture mechanics parameters of the elastic–plastic fracture mechanics, namely the J integral and the crack-tip opening displacement (CTOD). The CTOD values (δ_{dk}) describe the degree of deformation close to the crack tip and were calculated using the plastic-hinge model formally extended by replacing the total specimen deflection at maximum load (f_{max}) with the deflection at the notch tip region (f_k).

$$\delta_{dk} = \frac{1}{n} (W - a) \frac{4f_k}{s} \quad (1)$$

where W , a and s are the specimen width, the notch depth and the support span, respectively. The parameter n is a rotational factor and in our case $n = 4$.

The J value offers an energetic interpretation of the fracture behavior of the materials. In the present study the approximation method of Merkle and Corten [46] was used for obtaining the J -integral (J^{MC}). The J^{MC} value was calculated according to Eq. (2) and defined as resistance against unstable crack propagation.

$$J^{MC} = G + \frac{2}{B(W-a)} [D_1 A_G + D_2 A_K - (D_1 + D_2) A_{el}] \quad (2)$$

where

$$D_1 = \frac{1 + \gamma}{1 + \gamma^2} \quad D_2 = \frac{\gamma(1 - 2\gamma - \gamma^2)}{(1 + \gamma^2)^2} \quad \gamma = \frac{1456(W - a)}{s}$$

G is the energy release rate and A_G , A_K and A_{el} are the general deformation energy, the complementary energy and the elastic deformation energy up to maximum load, respectively. The procedure of instrumented impact testing used here is described very detailed by Grellmann and Seidler [47].

Furthermore, instrumented falling weight impact tests were performed in order to characterize the fracture behavior of the materials under triaxial loading, which represents the typical loading conditions applied on the components in the practice. The tests were carried out by means of a Impact Tester 5191 (JB Instruments), with a hemispherical tup (tip diameter of 20 mm), at impact velocity of ~ 4.5 m/s. Injection molded plates with dimensions length (L) \times width (W) \times thickness (B) of $120 \times 120 \times 2$ mm³ were tested at room temperature and at -20 °C.

The samples were positioned on a supporting ring with diameter of 40 mm. The total energy consumed (A) as well as the energy measured up to maximum load (A_G) was computed from the load-deflection diagrams and used for characterization of the material toughness. Further on, the ductility ratio (DR) was calculated according to Eq. (3)

$$DR = \frac{A - A_G}{A_G} \times 100\% \quad (3)$$

3. Results and discussion

3.1. Morphology

The morphology development of the investigated reactor blends as a function of EPC composition is extensively reported in another study of our group [44]. Typical heterophasic morphology was shown, consisting of EPC domains embedded in polypropylene matrix (Fig. 1). High ethylene content of EPC lead to the formation of crystallizable ethylene–propylene copolymer fractions. These are

incorporated as inclusions within the amorphous EPC domains, because of interfacial energy considerations (Fig. 1(a) and (b)). It was pointed out that the dispersed phase composition has the major influence on the matrix/dispersed phase compatibility of PP/EPC reactor blends. Increasing propylene content of the EPC results in an increasing chemical affinity between polypropylene matrix and propylene-rich dispersed phase and in an enhanced interfacial interaction, respectively. This was demonstrated by the shift of T_g^{EPC} and T_g^{PP} towards each other followed by a glass transition temperature merging phenomenon at extremely high propylene content of the dispersed phase (Table 1). The result strongly suggests that the propylene-rich dispersed phase is entrapped and partially dissolved in the amorphous region between PP lamellae. Furthermore, the enhanced compatibility results in a reduced interfacial tension of the dispersed phase against the matrix. Thus, a pronounced decrease of the dispersed domains size is observed with decreasing E_c^{EPC} (Table 1). It should be underlined that a reduction of the weight average particle diameter of several orders of magnitude took place solely as a function of the dispersed phase composition. However, despite the apparent homogeneity of the PP/EP17, suggested by the single glass transition, the material still demonstrates phase separation (Fig. 1(c)).

Parallel with the variation of the dispersed domain size, the EPC microstructure varies with the ethylene–propylene copolymer composition as well. At high ethylene content of EPC (> 50 wt%) both core–shell and ‘salami-like’ dispersed phase particles are observed, comprising amorphous shell with incorporated one or multiple polyethylene-like semi-crystalline inclusions, respectively (Fig. 1(a) and (b)). At very low E_c^{EPC} (< 30 wt%) it is assumed that long propylene sequences exist that can participate in the crystallization process of PP and probably to be incorporated in the polypropylene crystal lattice [44,48]. The effect of these morphological changes on the toughness and deformation behavior of the materials will be discussed below.

3.2. Tensile properties

The stress–strain curves of the investigated heterophasic copolymers are presented in Fig. 2. As shown the strain at

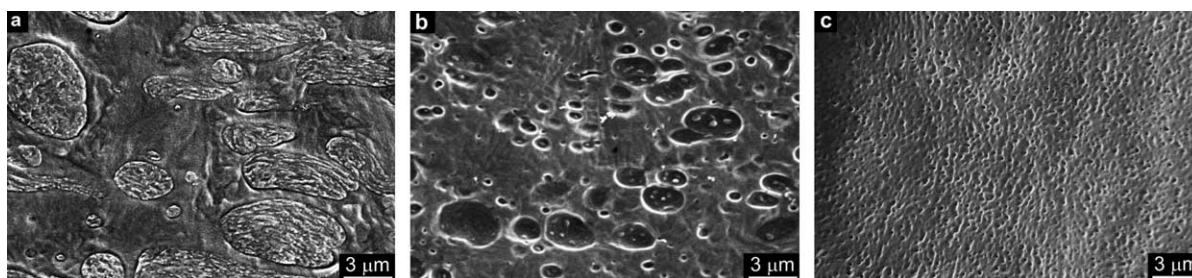


Fig. 1. SEM micrographs of: (a) PP/EP82, (b) PP/EP50, (c) PP/EP17.

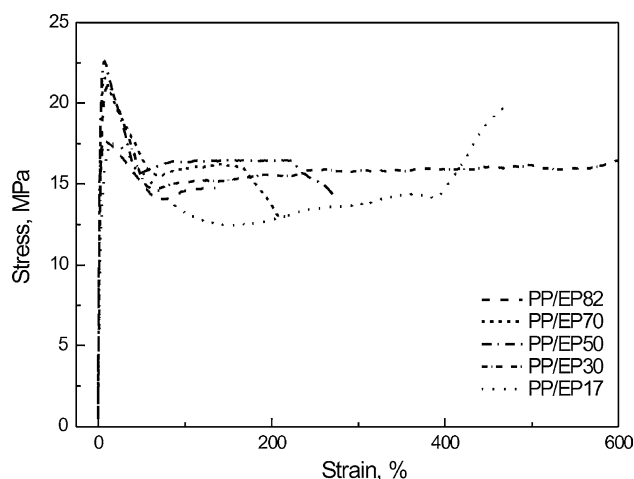


Fig. 2. Stress–strain behavior at room temperature of the heterophasic copolymers as a function of EPC composition.

break as a measure of the ductility increases with decreasing ethylene content of the EPC in compliance with the toughness increase, demonstrated by the instrumented Charpy measurements (Section 3.3). The enhanced compatibility between the matrix and the propylene-rich dispersed phase was considered as determinant for the observed phenomenon. However, the material PP/EP17 with the highest propylene content of the ethylene–propylene copolymer exhibits a slightly lower strain at break concomitant with a trend for strain hardening. As mentioned in Section 3.1, besides the preferential dissolution in the PP amorphous regions, some long propylene sequences of EP17 are considered capable in participating in the PP crystallization process and getting incorporated in the PP crystal lattice. In this sense the EP17 molecules can act as tie molecules [48] increasing the deformation resistance and thus leading to a strain hardening behavior. Further on, it should be considered that during the testing at room temperature both the dispersed phase and the matrix of PP/EP17 are already above their glass transition temperature, while for the other studied PP copolymers this temperature range corresponds to the glass transition region of polypropylene. Thus, the higher molecular mobility in PP/EP17 facilitates the rearrangement and alignment of the molecules parallel to the deformation direction, which is macroscopically detected as strain hardening phenomenon.

Fig. 3 shows the yield stress and the tensile modulus of the reactor blends as a function of the ethylene–propylene copolymer composition. Both curves exhibit the same behavior, passing through a maximum value at intermediate E_c^{EPC} . As previously reported [43,44], both the extremely high and extremely low ethylene containing EPC induce a suppression of the matrix crystallization process. This in turn results in a decrease of the crystallinity index of the heterophasic copolymers and accordingly in a diminution of stiffness and yield stress.

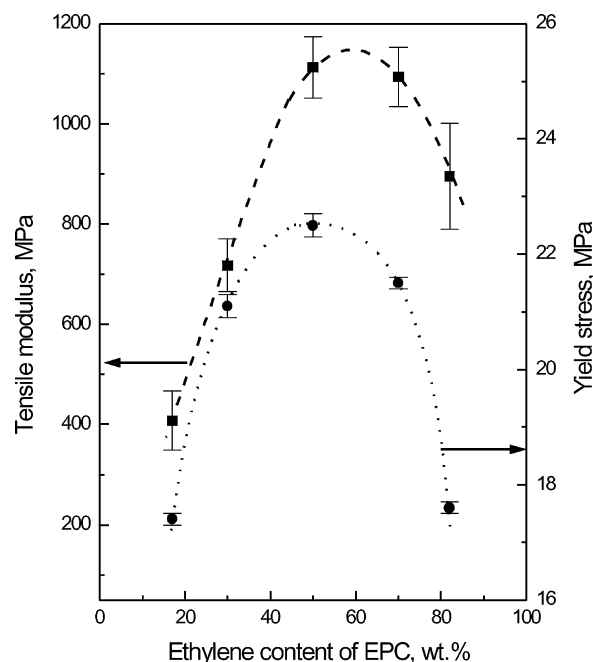


Fig. 3. Tensile modulus and yield stress at room temperature of the heterophasic copolymers as a function of EPC composition.

3.3. Fracture behavior

The load-deflection (F – f) diagrams recorded during the instrumented Charpy impact test were analyzed with respect to characteristic values of load, deflection and energy. Typical load-deflection curves of the polypropylene reactor blends as a function of test temperature are presented in Fig. 4. According to the results at 0 °C all the blends exhibit linear elastic behavior with brittle failure (Fig. 4(a)). By the increase of temperature a transition from elastic to elastic–plastic behavior characterized by a predominantly unstable crack growth was observed (Fig. 4(b)). Further increase of the temperature causes a second transition from predominantly unstable crack growth to predominantly stable crack growth accompanied with incomplete fracture of the specimens (Fig. 4(c) and (d)). The toughness increase over the temperature is clearly demonstrated by an increase of both J^{MC} and δ_{dk} values of the heterophasic copolymers (Figs. 5–7). As shown in Figs. 6 and 8 irrespective of the E_c^{EPC} , all the materials exhibit brittle behavior at low temperatures due to the moderate EPC weight fraction. However, a systematic enhancement of the fracture toughness at room temperature is observed with decreasing ethylene content of the ethylene–propylene copolymer. The effect is attributed to the enhanced compatibility, i.e. enhanced interaction between the polypropylene matrix and the propylene-rich dispersed phase. Further on, the refinement and more uniform spatial distribution of the dispersed EPC domains with decreasing ethylene content contribute to the higher toughness as well. The use of the conventional notched impact strength (Fig. 9) as a measure of the toughness seems to give comparable results but is methodically questionable as described in the chapter

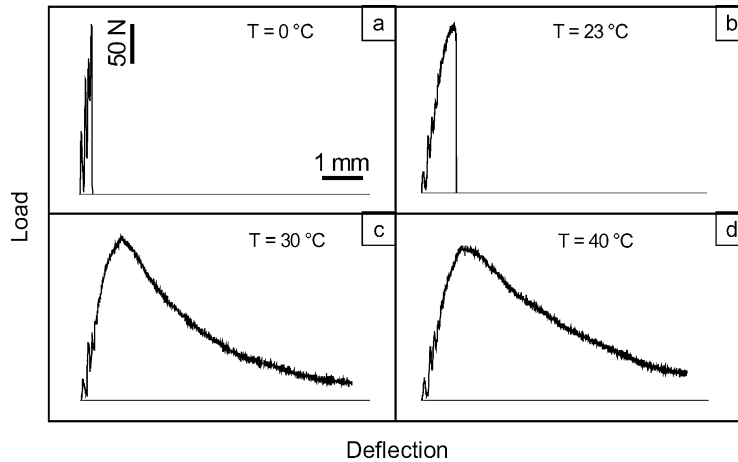


Fig. 4. Typical load-deflection diagrams of the heterophasic copolymers as a function of test temperature: (a) elastic behavior, unstable crack growth, (b) elastic–plastic behavior, unstable crack growth, (c) transition from unstable to stable crack growth, (d) stable crack growth.

‘brittle-to-tough transition’. Besides the macroscopic morphology changes, the ethylene–propylene copolymer composition controls also the microstructure of the dispersed EPC domains (Fig. 1). At high ethylene content, composite EPC particles comprised of amorphous shell with incorporated polyethylene-like semi-crystalline inclusions are observed. The number and size of the inclusions was found to correlate with the ethylene content of the EPC. Although the presence of polyethylene-like inclusions is advantageous for increasing EPC stiffness and producing low blush materials, after a certain volume fraction of inclusions the stress distribution around the dispersed particles is significantly modified [49]. For the studied materials, the role of the composite EPC particles with ethylene content above 70 wt% as stress

concentrators and impact modifiers is highly impaired because of the existence of a very large semi-crystalline polyethylene-like core. This leads to a poor toughness as shown in Fig. 5.

Further on, instrumented falling weight impact test (IFWI) was utilized in order to assess the fracture behavior of the heterophasic ethylene–propylene copolymers under triaxial loading.

Since these are the typical loading conditions applied on the components in practice, the IFWI is commonly used in the industry for material ranking. The tests were performed at room temperature and at -20 °C ; the results are summarized in Table 2. The same trend of increasing toughness at room temperature, represented by total energy consumption during perforation, was observed with decreasing E_c^{EPC} . However, at

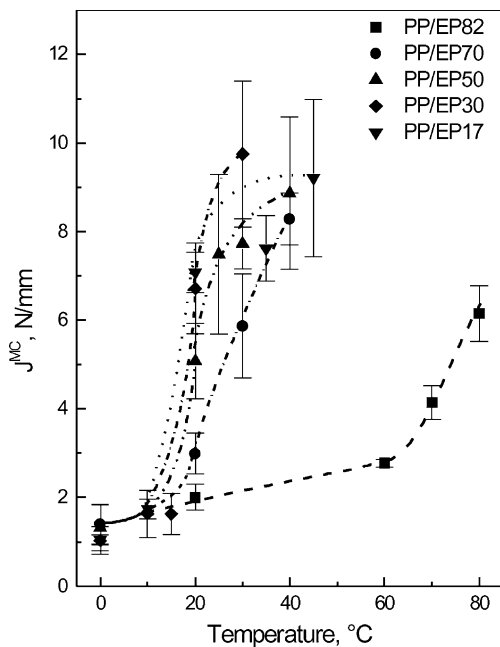


Fig. 5. Resistance against unstable crack propagation (J^{MC}) of the heterophasic copolymers as a function of temperature and EPC composition.

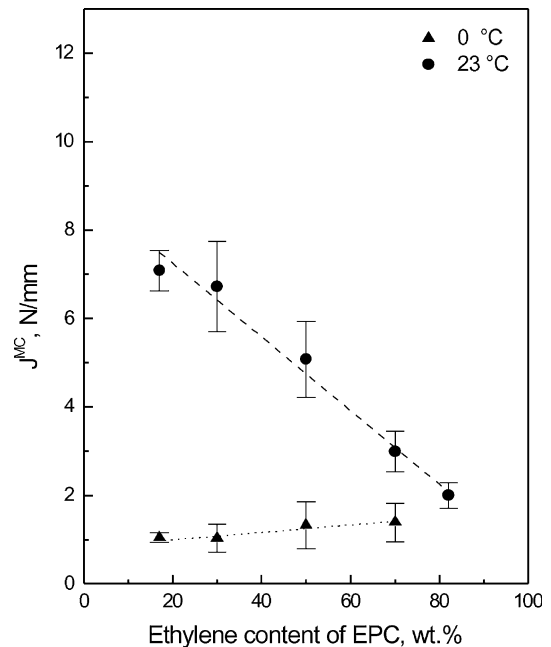


Fig. 6. Resistance against unstable crack propagation (J^{MC}) at 0 °C and room temperature as a function of EPC composition.

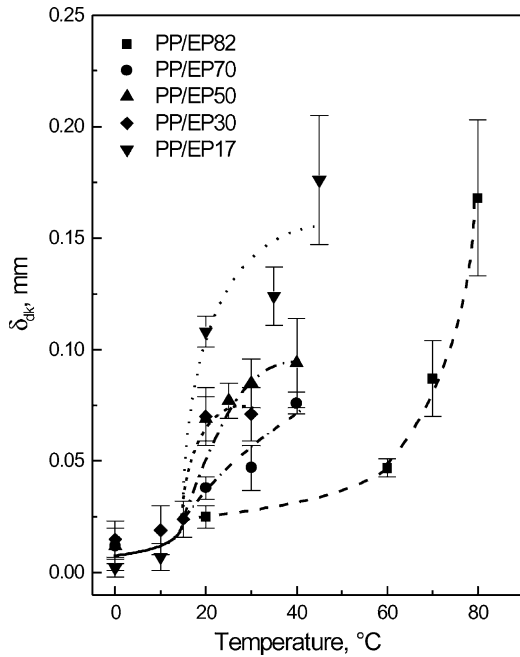


Fig. 7. Crack-tip opening displacement (δ_{dk}) of the heterophasic copolymers as a function of temperature and EPC composition.

–20 °C the toughness passes through a maximum value at average ethylene contents. Controlling matrix/dispersed phase compatibility of PP/EPC reactor blends by variation of the dispersed phase composition results in a variation of the glass transition temperature of the EPC phase as well (Table 1). Namely, enhancement of the matrix/dispersed phase compatibility by decreasing E_c^{EPC} produces a shift of T_g^{EPC} towards higher temperatures which in turn has a

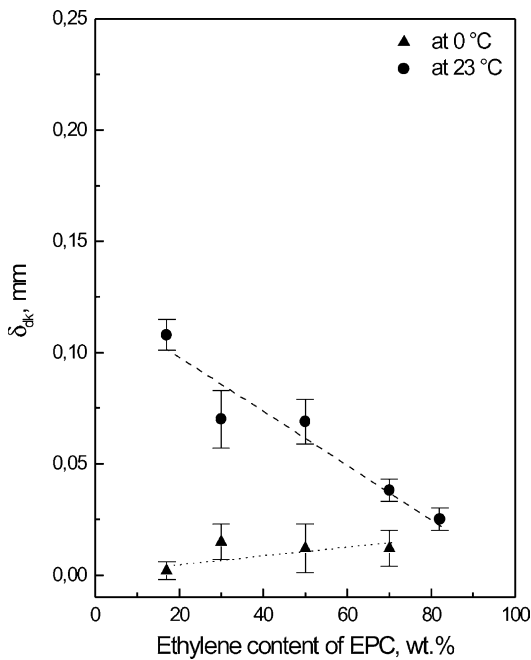


Fig. 8. Crack-tip opening displacement (δ_{dk}) at 0 °C and room temperature as a function of EPC composition.

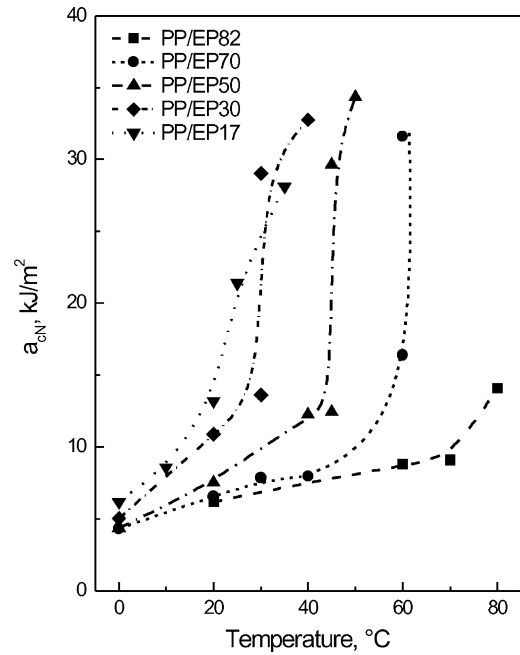


Fig. 9. Conventional notch impact strength (a_{cN}) of the heterophasic copolymers as a function of temperature and EPC composition.

detrimental effect on the impact strength at low temperatures. The material PP/EP17 displays the lowest toughness at –20 °C, because at this temperature the dispersed phase is already below its glass transition temperature acting as hard spheres with no stress concentration effect.

Moreover, the particle dimension was found also to play an important role. According to Jang et al. [30] bigger particles ($>0.4 \mu\text{m}$) are more effective in initiating matrix crazing in PP/EPDM blends, which is recognized as the main toughening mechanism in PP at low temperatures. However, as mentioned above, the existence of large polyethylene-like inclusions and the extremely coarse texture at very high ethylene contents have a negative influence on the low temperature impact strength as well.

3.4. Brittle-to-tough transition

It is known that in elastomer toughened systems and particularly in impact modified polypropylene a sharp increase of the toughness is observed with increasing test

Table 2
Instrumented falling weight impact properties

Materials	Test temperature: +23 °C		Test temperature: –20 °C	
	Total energy, A (J)	Ductility ratio, DR (%)	Total energy, A (J)	Ductility ratio, DR (%)
PP/EP82	21.1	31	19.4	21
PP/EP70	26.2	40	23.8	49
PP/EP50	27.5	48	28.7	71
PP/EP30	30.9	79	22.8	46
PP/EP17	28.4	134	1.1	5

temperature. The phenomenon is associated with a change in the deformation mechanisms as well as in the crack propagation mode and is designated as brittle-to-tough transition (BTT). The brittle-to-tough transition temperature (T_{BTT}) is most commonly obtained by means of conventional Charpy tests. However, the notched impact strength, as an integral quantity allows no separate evaluation of the resistance against stable crack initiation as well as unstable and stable crack propagation. The advantage of using the fracture mechanics concepts were pointed out by Grellmann et al. in Ref. [34], where by means of instrumented Charpy test the occurrence of two transitions was disclosed in PP/EPC materials. A ‘brittle/tough’ transition, which characterizes the resistance of the materials against unstable crack propagation and a ‘tough/high impact’ transition, describing the material’s resistance against stable crack propagation. While the former is initiated by the transition from unstable to stable crack growth, the ‘tough/high impact’ transition should be dominated by a transition in the deformation mechanism. On the basis of the conventional Charpy test such kind of material characterization is not possible. For the studied materials, the brittle-to-tough transition is demonstrated by a sharp increase of the J^{MC} and δ_{dk} (Figs. 5 and 7) values as a function of the temperature and is defined as a resistance against unstable crack propagation. The T_{BTT} was determined at the average value of the high and low plateau values of toughness. For comparative reasons the brittle-to-tough transition was obtained from the conventional notched Charpy impact test as well. However, it should be emphasized that the absolute values of the T_{BTT} obtained by the different methods are quite different. It comes on the one hand from the fact that the notched impact strength, in contrast to the J^{MC} and δ_{dk} values, is geometry dependent. On the other hand, the a_{cN} value reflects the notch sensitivity effects [50]. Thus, the notched impact strength allows no conservative assessment of the fracture behavior of the materials.

The brittle-to-tough temperatures of the heterophasic copolymers determined by the different approaches are presented in Fig. 10. The T_{BTT} values show a pronounced decrease with decreasing ethylene content of the dispersed phase irrespective if obtained by instrumented or conventional Charpy test. However, the brittle-to-tough transition temperatures determined by the instrumented impact test appear lower than these defined by means of conventional one, especially at intermediate E_c^{EPC} . The run of the curves varies with respect to the T_{BTT} determination approach as well. Taking into account the above mentioned principle differences of the instrumented and conventional impact test, the observed discrepancies in the brittle-to-tough transition are understandable. For the materials studied, the instrumented Charpy test was shown to be more sensitive method for T_{BTT} determination than the conventional one.

Generally, the brittle-to-tough transition in elastomer-modified systems occurs in the temperature region between

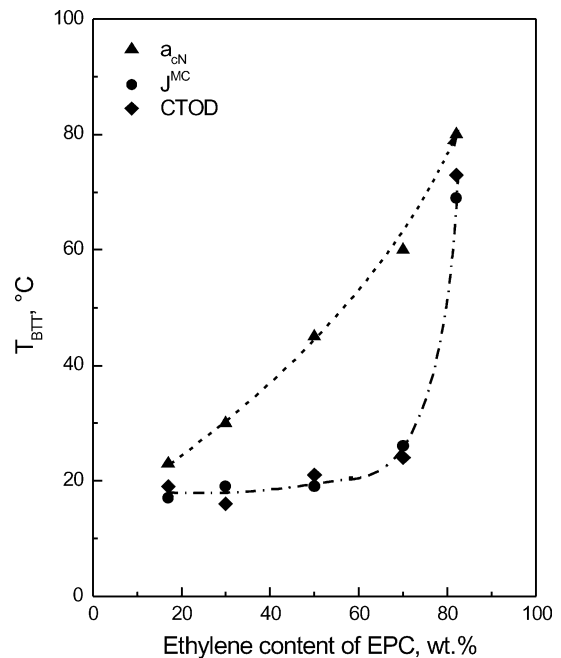


Fig. 10. Brittle-to-tough transition temperature (T_{BTT}) of the heterophasic copolymers as a function of EPC composition.

the T_{BTT} of the matrix and glass transition temperature of the modifier phase, while the latter serves as a lower limit. Under its glass transition temperature the elastomer phase behaves like solid particles and does not provide the necessary dispersed phase/matrix stiffness difference required to induce a stress concentration and to promote toughening effect, respectively. According to the critical interparticle distance theory proposed by Wu [19], the position of the brittle-to-tough transition in polymer blends is mostly dispersion dominated. However, this is valid only above the glass transition temperature of the elastomer component. The T_{BTT} of the studied materials as a function of the EPC particle diameter is shown in Fig. 11. Taking into account that the EPC weight fraction of the investigated

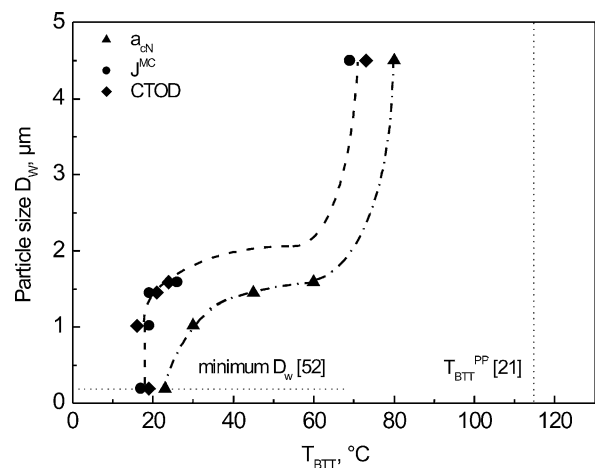


Fig. 11. Brittle-to-tough transition temperature (T_{BTT}) of the heterophasic copolymers as a function of the dispersed particle diameter.

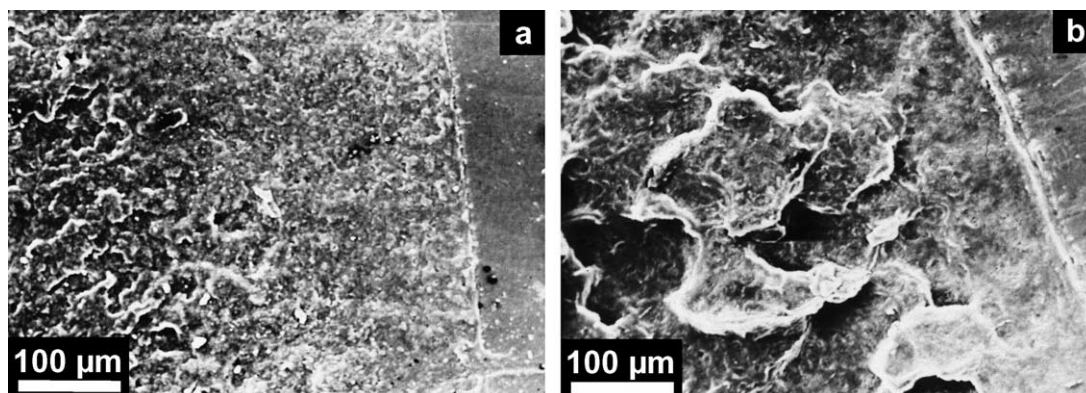


Fig. 12. SEM micrographs of fracture surfaces from PP/EP50 tested at 0 °C (a) and 30 °C (b).

materials was kept nearly constant, the observed reduction of the dispersed particle size with decreasing E_c^{EPC} corresponds to a reduction of the interparticle distance as well. However, it should be emphasized that the parallel variation of the both parameters impedes the separate determination of critical interparticle distance for a given particle size as well as the critical particle size for a given interparticle distance. As demonstrated in Fig. 11 the T_{BTT} determined by both instrumented and conventional Charpy tests exhibit the same dependence on the dispersed particle size. The instrumented Charpy, however, brings lower T_{BTT} values for a certain particle size as also reported by Starke et al. [33]. The materials with E_c^{EPC} above 30 wt%, exhibit a T_{BTT} dependence on the particle size, i.e. interparticle distance in compliance with the results of other authors [20, 21]. However, at lower ethylene concentrations the BTT appears not to be so susceptible to particle size variation. The fact is ascribed to the considerable increase of the glass transition temperature of the EPC phase at this composition region (Table 1). As discussed above, this would lead to a shift of the BTT lower limit towards higher temperatures. By approaching the T_g of the elastomer phase the BTT dependence on the particle size changes its character and a minimum BTT is reached for a certain ethylene–propylene copolymer composition. The effect is exemplified by the PP/EP17 material, where the lowest limit of T_{BTT} for this EPC composition is assumed to be reached.

Moreover, the existence of lower limit in the elastomer particle size for a certain composition has been reported in the literature as well [51–53]. The role of the very fine particles as impact modifiers is highly impaired, because they have high cavitation stress and thus are ineffective in triggering crazing. The lower limit of the particle size is a parameter characteristic for a given matrix. For polypropylene that was found to be $\sim 0.2 \mu\text{m}$ [53], this corresponds to the particle size in the material PP/EP17. Approaching the lower limit of the particle size is assumed to have a similar effect on the brittle-to-tough transition development as by approaching the elastomer T_g , namely giving a rise of a minimum T_{BTT} value for a certain elastomer composition.

It can be concluded that the T_{BTT} of the studied heterophasic materials is a complex result of the size, spatial packing and glass transition temperature of the dispersed elastomer particles.

Keeping in mind that in our case both the T_g and the particle size of the EPC are functions of its composition, it is suggested that the critical interparticle distance (ID_c), proposed by Wu to be the main parameter governing the BTT is characteristic not only for a given matrix but depends also on the intrinsic properties of the dispersed phase. Other researchers have also pointed out that the mechanical properties of the modifier phase have an important effect on the blend toughness and brittle-to-tough transition temperature [21,22].

3.5. Deformation mechanisms

The morphology and the deformation behavior at the notch tip of the materials during the impact test were investigated by means of scanning electron microscopy. The samples tested at 0 °C exhibit smooth fracture surfaces and broke in brittle manner with no signs of stress whitening (Fig. 12(a)). Most of the reactor blends showed the presence

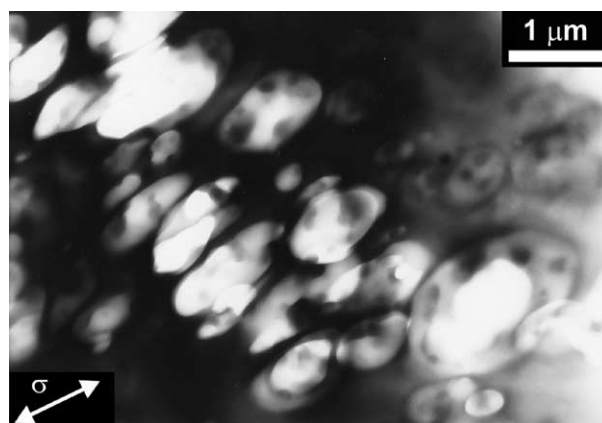


Fig. 13. HVEM micrograph of the initial deformation stage of PP/EP50 material disclosing the cavitation process. The arrow indicates the applied stress direction.

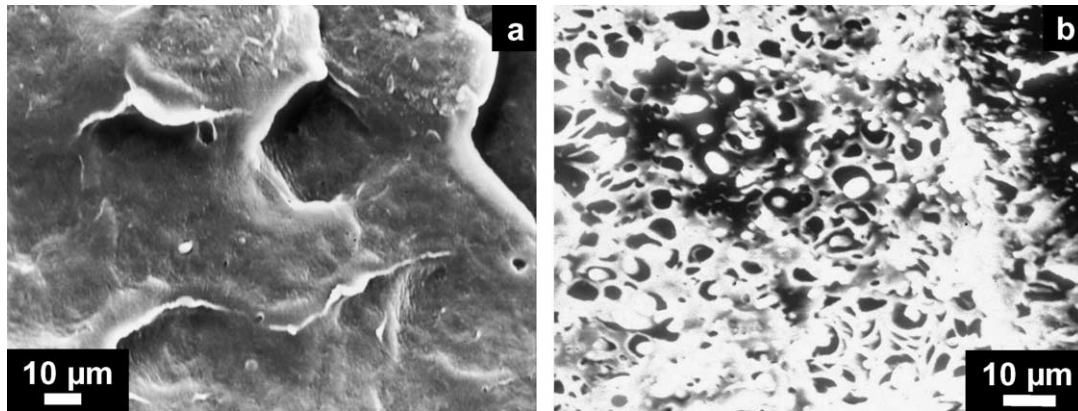


Fig. 14. SEM micrographs of fracture surfaces from PP/EP17 (a) and PP/EP70 (b) tested at 20–30 °C.

of debonded EPC particles on the fracture surface, suggesting poor adhesion and that the fracture front passed preferentially through particle-matrix interface. This was not the case for PP/EP17, where no debonded particles can be discerned indicating that the debonding stress of the particles is higher than the cleavage stress, i.e. rather good adhesion. Indeed, that did not lead to better impact properties, because of the high glass transition temperature of this material. At higher temperatures the materials reveal a wavy-like structure associated to a more ductile response (Fig. 12(b)). Initially a cavitation takes place within the dispersed phase particles as well as at the particle/matrix interface (Fig. 13). Kim et al. [15,16] pointed out that the internal cavitation process is facilitated by the presence of multiple inclusions in the EPC domains.

For the studied materials that is at E_c^{EPC} above 50 wt%. The cavitation is macroscopically represented as stress-whitening phenomenon. However, no cavitation and, respectively, no stress-whitening are observed in the material PP/EP17, suggesting the main deformation mechanism to be diffuse shear yielding (Fig. 14(a)). The effect is attributed to the increase of the cavitation stress with decreasing particle size [12] and to the high matrix/dispersed phase adhesion. On the contrary, the materials with high ethylene content show enhanced density and size of the voids (Fig. 14(b)). However, this fact did not produce an increase in the fracture parameters as reported by other authors [17]. The macrovoid nucleation process itself does not absorb the applied external mechanical energy. The main contribution for improving the toughness is suggested to be accomplished by interaction of neighboring voids forming dilatational bands and inducing shear deformation of the matrix material in the ligaments.

Further on, the stabilization of the dilatational band propagation and therewith delaying strain localization and premature failure are recognized to be of primary importance for the toughening process. Lazzeri [26] suggested that decreasing interparticle distance enhances the stability of dilatational band propagation leading to higher toughness, thus offering an alternative to the Wu

theory. In the materials studied, the cavity coalescence process and the subsequent stabilization of the dilatational bands are found to be dependent on the EPC composition and the test temperature. At intermediate temperatures the dilatational bands also designated by some authors as craze-like bands or croids occur only locally producing shear in the surrounding PP matrix. The propagation of the dilatational bands takes place predominantly in the interspherulitic regions of the reactor blends (Fig. 15). At further increase of the temperature, associated with the brittle-to-tough transition, the interaction between the voids becomes more intensive inducing diffuse shear yielding of the matrix accompanied with high degree of stress whitening of the whole fracture surface (Fig. 16).

Moreover, the EPC composition as a main factor controlling the matrix/dispersed phase compatibility and the dimension and interparticle distance of the dispersed domains influence the deformation processes as well. The increase of the toughness and decrease of the T_{BTT} with decreasing ethylene content of the EPC are thus associated with a decrease of the temperature of voids percolation onset and stabilization of the dilatational band propagation initiated by the better interfacial adhesion and finer

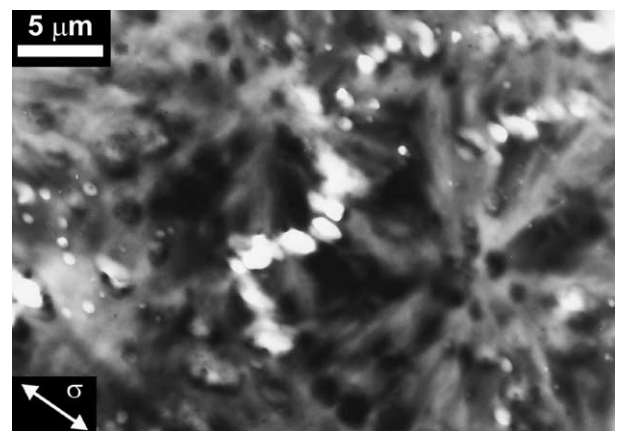


Fig. 15. HVEM micrograph of the cavity percolation onset of PP/EP50 material.

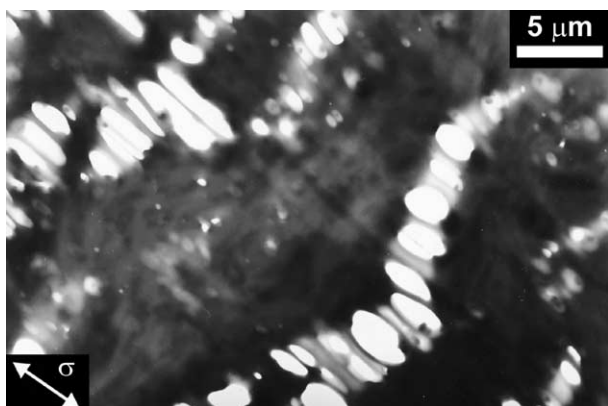


Fig. 16. HVEM micrograph of the intensive dilatational band formation stage of PP/EP50 material.

dispersion of the ethylene–propylene copolymer. Moreover, when above its glass transition temperature, the material PP/EP17 deforms directly by shear yielding without preliminary cavitation and dilatational band formation steps.

4. Conclusions

The fracture characteristics and deformation behavior of polypropylene/ethylene–propylene copolymer reactor blends have been investigated as a function of EPC composition. The enhanced matrix/dispersed phase compatibility and the underwent refinement of the dispersed phase domains with decreasing ethylene content of the ethylene–propylene copolymer was found to induce a systematic increase of the reactor blends toughness in the temperature range from 0 to 80 °C. Concomitantly, the T_{BTT} decreases in accordance with the observed reduction of the particle size and interparticle distance. However, this dependence is not linear and was found to be influenced significantly by the dispersed phase composition, suggesting that ID_c is not the only factor dominating the brittle-to-tough transition. The impact strength at lower temperatures, as shown by the instrumented falling weight measurements, is predominantly influenced by the glass transition temperature of the dispersed phase. Since increasing matrix/dispersed phase compatibility results in a parallel increase of the T_g^{EPC} an optimal property balance should be found. Indeed, for the materials studied the toughness at -20 °C exhibits a maximum value at intermediate ethylene contents of the EPC. The same trend is observed for the tensile modulus and the yield stress and is attributed to the suppression of the PP crystallization process both by extremely high and extremely low ethylene containing dispersed phase.

The main deformation mechanism observed in the studied heterophasic copolymers is related to the cavitation of the dispersed phase particles followed by percolation of the neighboring voids in form of cavitation (dilatational) bands. Below the brittle-to-tough temperature only isolated

cavitation bands appear on the fracture surfaces, while above the T_{BTT} the interaction between the voids becomes more intensive inducing diffuse shear yielding of the matrix. The improvement of the interfacial adhesion as well the decrease of the particle diameter and interparticle distance with decreasing EPC ethylene content was found to shift the void percolation onset to lower temperatures and to contribute for the stability of dilatational band propagation. Finally, the material PP/EP17 with the lowest ethylene content of the dispersed phase deforms directly by shear yielding without the preliminary cavitation and dilatational band formation steps.

Acknowledgements

The financial support of the State Government of Sachsen-Anhalt and the Dow Olefinverbund GmbH, Germany is gratefully acknowledged. The authors would like to thank D. Wulff and M. Hohlbein at Dow Olefinverbund GmbH (Schkopau, Germany) for producing the materials and performing the instrumented falling weight impact tests, respectively. Thank are due to M. Krumova and V. Seydewitz for carrying out the in situ deformation tests as well as S. Henning and C. Wicke for the SEM investigations.

References

- [1] Martuscelli E. In: Karger-Kocsis J, editor. Polypropylene structure, blends and composites. London: Chapman & Hall; 1995. p. 95.
- [2] Stricker F, Thomann Y, Muelhaupt R. J Appl Polym Sci 1998;68: 1891.
- [3] Da Silva ALN, Rocha MCG, Coutinho FMB, Bretas RES, Farah M. Polym Test 2002;21:647.
- [4] Arranz-Andres J, Benavente R, Pena B, Perez E, Cerrada M. J Polym Sci, Polym Phys 2002;B40:1869.
- [5] van der Ven S. Polypropylene and other polyolefins. New York: Elsevier; 1990 p. 268.
- [6] Albizzati E. In: Moore EP, editor. Polypropylene handbook. Munich: Carl Hanser; 1998. p. 89.
- [7] Mirabella F. Polymer 1993;34:1729.
- [8] Zagur R, Goizueta G, Capiati N. Polym Eng Sci 1999;39:921.
- [9] Hongjun C, Xiaolie L, Dezhu M, Jianmin W, Hongsheng T. J Appl Polym Sci 1999;71:93.
- [10] Michler GH. J Macromol Sci, Phys 1999;B38:787.
- [11] Michler GH. Kunststoff-Mikromechanik: Morphologie, Deformations- und Bruch-mechanismen. Muenchen Wien: Carl Hanser; 1992 p. 185.
- [12] Lazzeri A, Bucknall CB. Polymer 1995;36:2895.
- [13] Zebarjad SM, Lazzeri A, Bagheri R, Seyed Reihani SM, Frounchi M. Mater Lett 2003;57:2733.
- [14] Zebarjad SM, Bagheri R, Seyed Reihani SM, Lazzeri A. J Appl Polym Sci 2003;90:3767.
- [15] Kim GM, Michler GH. Polymer 1998;39:5689.
- [16] Kim GM, Michler GH, Gahleitner M, Fiebig J. J Appl Polym Sci 1996;60:1391.
- [17] Ferrer-Balas D, MasPOCH ML, Mai YW. Polymer 2002;43:3083.
- [18] Liang JZ, Li RKY. J Appl Polym Sci 2000;77:409.
- [19] Wu S. Polymer 1985;26:1855.

- [20] Borggreve RJM, Gaymans RJ, Schuijjer J, Ingen Housz JF. *Polymer* 1987;28:1489.
- [21] Jiang W, Liu C, Wang Z, An L, Liang H, Jiang B, et al. *Polymer* 1998;39:3285.
- [22] Borggreve RJM, Gaymans RJ, Schuijjer J. *Polymer* 1989;30:71.
- [23] van der Sanden MCM, de Kok JMM, Meijer HEH. *Polymer* 1994;35:2995.
- [24] Margolina A, Wu S. *Polym Commun* 1990;31:1995.
- [25] Jiang W, Tjong SC, Li RKY. *Polymer* 2000;41:3479.
- [26] Margolina A, Wu S. *Polymer* 1988;29:2170.
- [27] Lazzeri A. *Proceedings of 10th international conference on deformation, yield and fracture of polymers*. Cambridge, UK 1997 p. 75.
- [28] Danesi S, Porter R. *Polymer* 1978;19:448.
- [29] Stehling F, Huff T, Stanley Speed C, Wissler G. *J Appl Polym Sci* 1981;26:2693.
- [30] Jang BZ, Uhlmann DR, van der Sande JB. *J Appl Polym Sci* 1985;30:2485.
- [31] Ramsteiner F. *Acta Polym* 1991;42:584.
- [32] van der Wal A, Verheul AJJ, Gaymans RJ. *Polymer* 1999;40:6057.
- [33] Starke JU, Michler GH, Grellmann W, Seidler S, Gahleitner M, Fiebig J, et al. *Polymer* 1998;39:75.
- [34] Grellmann W, Seidler S, Jung K, Kotter I. *J Appl Polym Sci* 2001;79:2317.
- [35] Koch T, Seidler S, Jung K, Grellmann W. In: Grellmann W, Seidler S, editors. *Deformation and fracture behaviour of polymers*. Berlin: Springer; 2001. p. 257.
- [36] Yokoyama Y, Ricco T. *Polymer* 1998;39:5689.
- [37] Grein C, Bernreitner K, Hauer A, Gahleitner M, Neissl W. *J Appl Polym Sci* 2003;87:1702.
- [38] D'Orazio L, Mancarella C, Martuscelli E, Polato F. *Polymer* 1991;32:1186.
- [39] Kim BK, Do IH. *J Appl Polym Sci* 1996;61:439.
- [40] Nomura T, Nishio T, Fujii T, Sakai J, Yamamoto M, Uemura A. *Polym Eng Sci* 1995;35:1261.
- [41] van der Wal A, Nijhof R, Gaymans RJ. *Polymer* 1999;40:6031.
- [42] Greco R, Mancarella C, Martuscelli E, Ragosta G, Jinghua Y. *Polymer* 1987;28:1929.
- [43] Doshev P, Lohse G, Henning S, Michler GH, Radosch HJ. *Proceedings of 20th annual meeting of Polymer Processing Society*, Akron, USA 2004 p. 298.
- [44] Doshev P, Lohse G, Henning S, Krumova M, Heuvelsland A, Michler GH, et al. Submitted for publication.
- [45] Olley RH, Hodge AM, Bassett DC. *J Polym Sci, Polym Phys* 1979;B17:627.
- [46] Merkle JG, Corten HT. *J Pressure Vessel Technol* 1974;6:286.
- [47] Grellmann W, Seidler S, editors. *Deformation and fracture behaviour of polymers*. Berlin: Springer; 2001.
- [48] Nitta K-H, Shin Y-W, Hashiguchi H, Tanimoto S, Terano M. *Polymer* 2005;46:965.
- [49] Ricco T, Pavan A, Danusso F. *Polym Eng Sci* 1978;18:774.
- [50] Huang L, Pei Q, Yuan Q, Li H, Cheng F, Ma J, et al. *Polymer* 2003;44:3125.
- [51] Donald AM, Kramer EJ. *J Appl Polym Sci* 1982;27:3729.
- [52] Gaymans RJ, Borggreve RJM, Oostenbrink AJ. *Macromol Chem, Macromol Symp* 1990;38:125.
- [53] Wei GX, Sue HJ. *Polym Eng Sci* 2000;40:1979.